

Enhanced infrared absorption of NiCr Film fabricated on LiTaO₃ crystal material for 14 ~ 16 μm application

LIU Zi-Ji*, LIANG Zhi-Qing*, HE Xuan, MA Zhen-Dong, GOU Jun, JIANG Ya-Dong

(State Key Laboratory of Electronic Thin Films and Integrated Devices,
University of Electronic Science and Technology of China, Chengdu 610054, China)

Abstract: Nano-scale metallic films have been proven to be effective infrared absorption layers for pyroelectric detectors operated at 14 ~ 16 μm spectral range for space applications. The infrared absorption improvement can be achieved by adjusting the thickness and surface characteristics of the nano-scale Nickel-chromium (NiCr) film deposited on the LT (lithium tantalite) crystal materials. By regulating the thickness of the crystal materials, the absorption wavelength is adjustable as well by changing the depth of the anti-reflection cavity. To enhance the infrared absorption further, chemical corrosion is applied on this film, which generates a rough nano-scale surface structure and greatly increases the absorption surface area. By combining these two methods, absorption at specified infrared wavelength could be distinctly enhanced, and the manufacturing process is fully compatible and easy to realize. Experiment results suggest that the absorption performance which could be controlled agrees well with the simulation and design.

Key words: NiCr, pyroelectric detector, nano-scale thin metallic films, chemical corrosion, infrared absorption

PACS: 85.25.Pb, 85.60.Gz

基于钽酸锂晶体材料镍铬薄膜在 14 ~ 16 μm 波段红外增强吸收特性

刘子骥*, 梁志清*, 何璇, 马振东, 苟军, 蒋亚东

(电子科技大学 电子薄膜与集成器件国家重点实验室, 四川 成都 610054)

摘要: 纳米级金属薄膜能够作为热释电探测器红外吸收薄膜在 14 ~ 16 μm 波段范围内有效应用已经得到证明. 通过调节沉积在 LT (钽酸锂) 晶体材料上的纳米级镍铬 (NiCr) 薄膜的厚度和表面特征来改善纳米金属薄膜红外吸收特性. 通过调节晶体材料的厚度, 改变抗反射腔的深度, 从而调节吸收波长. 为进一步加强红外吸收, 应用化学腐蚀, 生成粗糙的纳米级薄膜表面结构, 从而极大程度上增加吸收表面积. 通过将这两种方法结合, 可以明显增强指定波段的红外吸收, 且其制造过程完全兼容, 易于实现. 可控的吸收性能的实验结果与仿真和设计情况相符合.

关键词: NiCr; 热释电探测器; 纳米金属薄膜; 化学腐蚀; 红外吸收

中图分类号: O551, O782 文献标识码: A

Introduction

The infrared characteristics of thin metal films are attractive for security and medical applications due to their abilities to penetrate most dry, non-polar materials without damaging them^[1-2]. Nano-scale metallic films for infrared absorption have been shown to be usable for

effective detectors^[3-4]. In pyroelectric detectors, the radiation energy heats the sensing element, changing its polarization and producing an electrical output proportional to the incident optical power^[5]. However pyroelectric detectors provide a low sensitivity at infrared spectral range due to poor absorption of infrared radiation^[3]. To increase the sensitivity, despite the thermal isolation, it is necessary to design a pixel membrane absorption struc-

Received date: 2016-11-07, revised date: 2017-04-08

收稿日期: 2016-11-07, 修回日期: 2017-04-08

Foundation items: Supported by National Science Funds for Creative Research Groups of China (61421002), National Natural Science Foundation of China (61405027), the Postdoctoral Science Foundation of China (2014M562296), and Fundamental Research Funds for the Central Universities (ZYGX2011X012)

Biography: LIU Zi-Ji (1981-), male, Chongqing China. Ph. D. Research area involves pyroelectric detection and sensor technology.

* **Corresponding author:** E-mail: zliu@uestc.edu.cn, liangzq2012@126.com

ture to efficiently absorb infrared energy without compromising the pyroelectric proprieties of the sensors^[3,6]. Nanometer-scale metal films deposited on dielectric layers are known to provide good infrared absorption due to resistive losses in the film^[7-9]. In this paper, the infrared absorption characteristics of the nickel-chromium (NiCr) thin film which was deposited on the lithium tantalite crystal material with specific thickness as an infrared absorption layer are shown both theoretically and experimentally. A surface treatment process by chemical corrosion is first suggested to further enhance infrared absorption of NiCr film.

1 Theoretical analysis

In 1947, Hadley and Dennison predicted that an unsupported metal film in air could absorb 50% of incident infrared radiation at most^[10]. This optimum absorption can be achieved for a specific infrared spectral range through an appropriate combination of conductivity and thickness^[7-8]. To simplify the simulation model, the sensor element of the pyroelectric detector is depicted as a sandwich structure shown in Fig. 1.

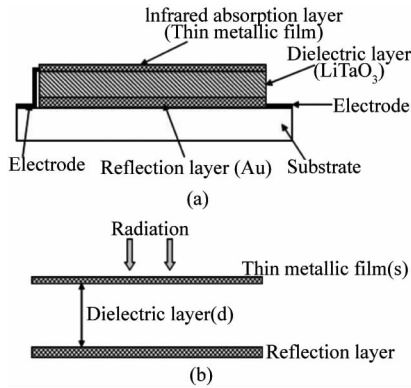


Fig. 1 Schematic cross-sectional view: (a) sensing element structure of a pyroelectric detector, (b) simplified optical resonance cavity structure

图1 横截面示意图(a)热释电探测器敏感元件结构,(b)简化光学谐振腔结构

In Fig. 1, s and d represent the thickness of metallic film and dielectric layer LiTaO₃ wafers respectively. In this analysis, only the electric field component perpendicular to the sensor plane (Fig. 1) is considered, since it is straightforward to the parallel component. For the structure depicted in Fig. 1(a)^[7-8,11], the coefficients transmission (T), reflection (R) and absorption (A) of the film satisfy the equation $A = 100 - (R + T)$, each one can be expressed as follows^[7], respectively.

$$R = \frac{\left[\left(\frac{4\pi k^2 s}{\lambda} + 1 - \frac{1}{n_3^2} \right)^2 \sin^2(k_3 d) + \frac{\left(\frac{16\pi^2 k^4 s^2}{\lambda^2} \right)}{n_3^2} \cos^2(k_3 d) \right]}{\left[\left(\frac{4\pi k^2 s}{\lambda} + 1 + \frac{1}{n_3^2} \right)^2 \sin^2(k_3 d) + \frac{4}{n_3^2} \left(1 + \frac{2\pi k^2 s}{\lambda} \right)^2 \cos^2(k_3 d) \right]}, \quad (1)$$

$$T = \frac{\frac{4}{n_3^2}}{\left[\left(\frac{4\pi k^2 s}{\lambda} + 1 + \frac{1}{n_3^2} \right)^2 \sin^2(k_3 d) + \frac{4}{n_3^2} \left(1 + \frac{2\pi k^2 s}{\lambda} \right)^2 \cos^2(k_3 d) \right]}, \quad (2)$$

$$A = \frac{\frac{\left(\frac{16\pi k^2 s}{\lambda} \right)}{n_3^4} \sin^2(k_3 d) + \frac{\left(\frac{16\pi k^2 s}{\lambda} \right)}{n_3^2} \cos^2(k_3 d)}{\left[\left(\frac{4\pi k^2 s}{\lambda} + 1 + \frac{1}{n_3^2} \right)^2 \sin^2(k_3 d) + \frac{4}{n_3^2} \left(1 + \frac{2\pi k^2 s}{\lambda} \right)^2 \cos^2(k_3 d) \right]}, \quad (3)$$

where k_m is the complex propagation constant with an incidence angle θ_m (in most applications $\cos\theta_m \approx 1$) on the m' th boundary, and it can be represented as $k_m = [2\pi n_m / \lambda] \cos\theta_m$, in which the n_m is the refraction of the m' th layer. For non-magnetic metal layers, the index of refraction and the extinction coefficient could be approximated as $\eta = \kappa = \sqrt{\sigma} / 2\omega\epsilon_0$, where σ represents the conductivity of metal, $\omega = 2\pi c / \lambda$ and ϵ_0 is the free space permittivity^[6]. Finally, the supporting layer ($m = 3$ in Fig. 1) is usually a dielectric with small losses, thus n_3 can be considered real. For pyroelectric detector, the LiTaO₃ crystal material film is usually used as the dielectric layer. The contributions for absorption could be neglected as the LT crystal exhibits small losses. So in the further analysis, the depth of this insulate layer is set to zero (i. e., $d = 0$). Based on the analysis above, the Eqs. 1-3 can be reduced to:

$$A = \frac{\frac{\sigma s}{c\epsilon_0}}{\left(1 + \frac{\sigma s}{2c\epsilon_0} \right)^2}, \quad (4)$$

$$R = \frac{\sigma^2 s^2}{4c^2 \epsilon_0^2 \left(1 + \frac{\sigma s}{2c\epsilon_0} \right)^2}, \quad (5)$$

$$T = \frac{1}{\left(1 + \frac{\sigma s}{2c\epsilon_0} \right)^2}. \quad (6)$$

The absorption analysis given in Eq. 4 only depends on the thin metallic film conductivity σ and its thicknesses, of which the conductivity is the inverse of the sheet resistance of the film. Furthermore, the absorption given in Eq. 4 depends only on the product of film conductivity and its thickness. In addition, since the conductivity of metal films is nearly constant at this frequency range^[12], absorption can be considered independent of frequency. From Eq. 4, it is easy to find that the maximum absorption occurs at $\sigma s = 2c\epsilon_0$. Figure 2 shows reflection, transmission and absorption as a function of thickness or conductivity, respectively, in case of 8.2 nm metal film and conductivity of 6.5×10^5 S/m. It is clearly shown that the maximum absorption is about 50%, when both the transmission and reflection are approximately equal to 25%. At this time, we can conclude that the maximum absorption can be achieved at the condition of 8.2 nm of

the metal thickness and 6.5×10^5 S/m of the film conductivity σ .

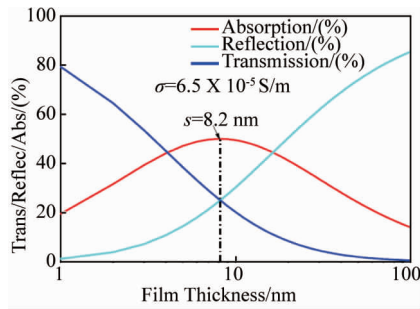


Fig. 2 Reflection, transmission and absorption of nano-scale metallic films as a function of thickness and conductivity of the film with Matlab simulation software
图2 纳米级金属薄膜反射、透射及吸收特性随厚度及导电性变化的 Matlab 仿真结果

For the specific wavelength absorption enhancement, we need to design resonance cavity depth. Figure 3 shows the calculated results of the thickness of cavity at 8.2 nm metal film and conductivity of 6.5×10^5 S/m. The simulations show that when the thickness of the resonance cavity (thickness of LT wafers) is 9.6 μm, the average absorption rate in the range of 14 ~ 16 μm is the best of 74.4%, where the peak absorption wavelength is about 15 μm. At the same condition, the average absorption between 14 μm to 16 μm is 43.2%, 60.9%, 69.8% respectively in case of 8 μm, 9 μm and 10 μm of LT layer.

2 Experimental results

Nano-scale NiCr (Ni:Cr = 80:20) films were deposited on the LiTaO₃ crystal slice of pyroelectric detector by magnetron sputtering of a high purity NiCr target in an Ar atmosphere. The two steps in the fabrication of making ultra-thin LT wafer are as follows: mechanical thinning processes and chemical corrosion. 50 μm LT wafer can be obtained by grinding and polishing a single-crystal 200 μm thick wafer. After cutting and chemical corrosion processes, the thickness of the LiTaO₃ sensitive layer could reach up to 9.6 μm^[13-14]. Films with different thicknesses from 10 nm to 40 nm were prepared at a specific thickness (9.6 μm) LT crystal material for 14 ~ 16 μm absorption enhancing. Since transmittance was negligible due to the reflection layer which was fabricated by magnetron sputtering high purity Au at about 200 nm. So, the absorption of the samples, $A(\lambda)$, can be calculated directly as $A(\lambda) = 100\% - R(\lambda)$ with the transmittance neglected, and the reflection $R(\lambda)$ can be measured by a Fourier transform infrared spectrometer (FTIR) directly.

Shown in Fig. 4 is the experimental reflection of nano-scale metallic films on the LiTaO₃ crystal slice with varying NiCr thicknesses prepared by magnetron sputtering and chemical corrosion. A reasonably good agreement between the estimation and measurements is observed, the absorption of the NiCr film increases with the decrease of metallic film thickness. It suggests that

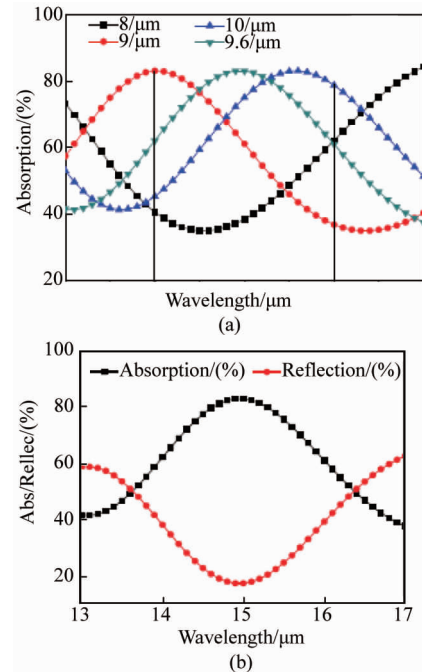


Fig. 3 (a) The calculation result of the absorption curves for 8 μm, 9 μm, 9.6 μm and 10 μm of LT layer, (b) the calculation result of the absorption curves and reflection curves for 9.6 μm of LT layer
图3 (a) LT层在 8 μm, 9 μm, 9.6 μm 及 10 μm 处的吸收曲线计算结果, (b) LT层在 9.6 μm 处的吸收及反射曲线计算结果

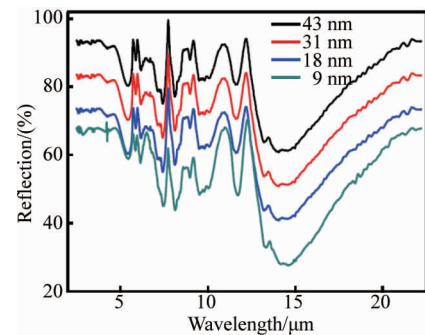


Fig. 4 The reflection of nano-scale metallic films on the LiTaO₃ crystal slice with varying NiCr thicknesses
图4 LiTaO₃ 晶体切片上纳米级金属薄膜反射特性随 NiCr 厚度变化的情况

the thickness of NiCr films plays an important role for the infrared absorption in this structure. The differences between the calculated absorptions and measurements for small thicknesses may be attributed to the porous structure of the film. The NiCr film, which becomes thinner due to its porous growth, has a smaller thickness compared with the value (10 nm) calculated by sputtering rate and time.

However, the infrared absorption of NiCr films can achieve a good value when it is simply integrated in a sensing element structure. After fabrication of the sensing element, a surface decoration by chemical corrosion to this metallic film can greatly increase the absorption surface

area. Strong oxidizing solution (H_2O_2) mixed with KOH was used to etch the polished $LiTaO_3$ crystal^[13]. It can be seen that an effectively enhanced absorption by the chemical corrosion treatment can be observed from Fig. 5.

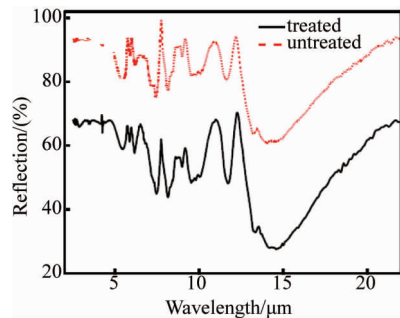


Fig. 5 Absorptions of untreated thin metallic film (dashed line) and chemical corrosion treated thin metallic film (solid line) with a NiCr thickness of 10 nm

图5 未经处理的金属薄膜(虚线)和经化学腐蚀后的金属薄膜(实线)在NiCr厚度为10 nm时的吸收情况

The experimental results are shown in Fig. 6, in which a specific thickness film is fabricated from a 50 nm NiCr film by chemical corrosion. It becomes clear that the effective surface area can be increased due to porous structures. It is also known that the absorption $A(\lambda)$ consists of two components^[15-16]: $A(\lambda) = A_{INTR}(\lambda) + A_{SS}(\lambda)$, where $A_{INTR}(\lambda)$ is the intrinsic absorption of an ideally smooth surface on a specific thickness LT crystal material, and $A_{SS}(\lambda)$ is the contribution due to porous surface structures, which are induced by chemical corrosion process in this paper. The influence of porous structure on the surface structure absorption $A_{SS}(\lambda)$ needs more investigations in further research. The sample preparation process of $LiTaO_3$ crystal slice thinning and nano-scale metallic films is a physical process, which has a good repeatability. The experimental conditions of chemical corrosion process is easy to control, so the sample preparation process also has a good repeatability.

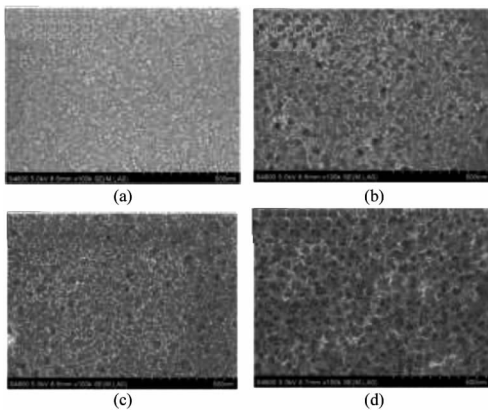


Fig. 6 SEM images of NiCr films: (a) an untreated thin metallic films surface, and a chemical corrosion treated thin metallic films surface (b)31 nm, (c)18 nm, (d)9 nm

图6 NiCr薄膜的SEM图像(a)未被处理的金属薄膜表面及经化学腐蚀处理的金属薄膜表面, (b)31 nm, (c)18 nm, (d)9 nm

3 Conclusions

Infrared absorption characteristics of pyroelectric detectors coupled with metallic films and LT crystal materials were analyzed and measured. Porous nano-scale NiCr films with varying thicknesses were deposited on a LT crystal material. A reasonably good agreement between the measurements and calculations suggests that the NiCr film acts as an effective infrared absorption layer in the porous nano-scale surface structures. To achieve a higher responsivity for the detector, an additional process by chemical corrosion could effectively improve the infrared absorption characteristics due to the porous nano-scale structures on metallic film surface.

References

- [1] Bjarnason J E, Chan T L J, Lee A W M, *et al.* Millimeter-wave, terahertz, and mid-infrared transmission through common clothing[J]. *Applied Physics Letters*, 2004, **85**(4):519-521.
- [2] Wallace V P, Taday P F, Fitzgerald A J, *et al.* Terahertz pulsed imaging and spectroscopy for biomedical and pharmaceutical applications. [J]. *Faraday Discussions*, 2003, **126**(2):255-263.
- [3] Advena D J, Bly V T, Cox J T. Deposition and characterization of far-infrared absorbing gold black films. [J]. *Applied Optics*, 1993, **32**(7):1136-1144.
- [4] Gou J, Wang J, Zheng X, *et al.* Detection of terahertz radiation from 2.52 THz CO2 laser using a 320×240 vanadium oxide microbolometer focal plane array [J]. *Rsc Advances*, 2015, **5**(102):84252-84256.
- [5] Peterson R L, Day G W, Gruzensky P M, *et al.* Analysis of response of pyroelectric optical detectors[J]. *Journal of Applied Physics*, 1974, **45**(8):3296-3303.
- [6] Grbovic D, Lavrik N V, Rajic S, *et al.* Arrays of SiO_2 substrate-free micromechanical uncooled infrared and terahertz detectors[J]. *Journal of Applied Physics*, 2008, **104**(5):647-581.
- [7] Alves F, Karamitros A, Grbovic D, *et al.* Highly absorbing nano-scale metal films for terahertz applications[J]. *Optical Engineering*, 2012, **51**(6):063801-1-063801-6.
- [8] Alves F, Karamitros A, Grbovic D, *et al.* Highly absorbing nano-scale metal films for terahertz[J]. *Proceedings of SPIE - The International Society for Optical Engineering*, 2011, **51**(6):351-353.
- [9] Bolakis C, Grbovic D, Lavrik N V, *et al.* Design and characterization of terahertz-absorbing nano-laminates of dielectric and metal thin films. [J]. *Optics Express*, 2010, **18**(14):14488-95.
- [10] Hadley L N, Dennison D M. Reflection and transmission interference filters. [J]. *Journal of the Optical Society of America*, 1947, **37**(6):451; passim.
- [11] Hilsom C. Infrared absorption of thin metal films[J]. *Opt. Soc. Am.* 1954, **44**(3):188-191.
- [12] Laman N, Grischkowsky D. Terahertz conductivity of thin metal films [J]. *Applied Physics Letters*, 2008, **93**(5):051105-051105-3.
- [13] Liang Z Q, Li S B, Liu Z J, *et al.* High responsivity of pyroelectric infrared detector based on ultra-thin (10 μm) $LiTaO_3$ [J]. *Journal of Materials Science: Materials in Electronics*, 2015, **26**(7):5400-5404.
- [14] Wang J, Gou J, Li W. Preparation of room temperature terahertz detector with lithium tantalate crystal and thin film[J]. *Aip Advances*, 2014, **4**(2):97-105.
- [15] Vorobyev A Y, Topkov A N, Gurin O V, *et al.* Enhanced absorption of metals over ultrabroad electromagnetic spectrum[J]. *Applied Physics Letters*, 2009, **95**(12):121106-121106-3.
- [16] Li X F, Zhang C Y, Li H, *et al.* Formation of 100-nm periodic structures on a titanium surface by exploiting the oxidation and third harmonic generation induced by femtosecond laser pulses[J]. *Optics Express*, 2014, **22**(23):28086-99.